

## **Thermal and Electrical Conductivities of an Improved 9 Cr-1 Mo Steel from 360 to 1000 K**

**R. K. Williams,<sup>1</sup> R. S. Graves,<sup>1</sup> and D. L. McElroy<sup>1</sup>**

*Received February 28, 1984*

---

The electrical and thermal conductivities and Seebeck coefficients of three 9 Cr-1 Mo samples were measured over the temperature range 360-1000 K. All of the samples were in the normalized and tempered condition and two of the samples were from different heats of a new, modified alloy. The thermal conductivity of the third sample, which was from a commercial heat, was found to agree well with the ASME code values for this steel. The two heats of modified 9 Cr-1 Mo were found to have significantly higher thermal conductivities and this difference appears to be due to the lower Si content of the modified alloy. The results were compared with the predictions of standard transport theory and data on bcc Fe. These comparisons show that phonon energy transport is important and quite dependent upon the Si content.

---

**KEY WORDS:** electrical resistivity; steels (Cr-Mo); thermal conductivity.

### **1. INTRODUCTION**

The results presented in this paper were obtained to define the thermo-physical properties of an improved 9 Cr-1 Mo steel. The new alloy has mechanical properties that exceed those of 304 stainless steel up to about 850 K, and was developed for applications in which thermal stresses are important [1]. The thermal conductivity  $\lambda$  is an important parameter in these applications and understanding the variations in  $\lambda$  from heat to heat and with temperature is required both for ASME code certification of the new alloy and for further development of ferritic steels. Fortunately, the

---

<sup>1</sup>Metals and Ceramics Division, Oak Ridge National Laboratory, Oak Ridge, Tennessee 37830, U.S.A.

new alloy has a higher  $\lambda$  than the older commercial 9 Cr-1 Mo composition, and identifying the factors responsible for this enhancement is the principal goal of this paper.

The measurements were made in a guarded absolute longitudinal heat flow apparatus that has been described previously [2] and recently tested with a standard material [3] over the full operating range, 360-1000 K. The analysis of the results is based on identifying the electron  $\lambda_e$  and phonon  $\lambda_p$  components of  $\lambda$ :

$$\lambda = \lambda_e + \lambda_p \quad (1)$$

and quantitatively identifying the scattering process that limits each component. This treatment is based on an earlier study of  $\lambda_e$  and  $\lambda_p$  in bcc Fe [4].

## 2. SAMPLE CHARACTERIZATION

Table I shows chemical analyses of the three heats studied. Two of the heats (30176 and 30394) were the modified alloy and contained V and Nb additions. The Si contents of these two heats were also considerably lower than that of the commercial heat (15965). The melting and fabrication practice has been described elsewhere [1]. All three heats were in the normalized (1310 K, 1 h; air cool) and tempered (1030 K, 1 h; air cool) condition. Extensive investigations [1, 5] have shown that this heat treat-

Table I. Chemical Analysis of Three Heats of 9 Cr-1 Mo Steel<sup>a</sup>

| Element | Heat 15965<br>(commercial) | Heat 30176<br>(modified) | Heat 30394<br>(modified) |
|---------|----------------------------|--------------------------|--------------------------|
| Cr      | 9.38                       | 8.41                     | 8.35                     |
| Mo      | 0.99                       | 0.90                     | 1.03                     |
| C       | 0.11                       | 0.075                    | 0.084                    |
| Si      | 0.71                       | 0.19                     | 0.45                     |
| Mn      | 0.59                       | 0.40                     | 0.47                     |
| V       | 0.054                      | 0.204                    | 0.202                    |
| Nb      | 0.010                      | 0.072                    | 0.080                    |
| Ni      | 0.07                       | 0.10                     | 0.09                     |
| Ti      | 0.002                      | 0.004                    | 0.005                    |
| Co      | 0.081                      | 0.016                    | 0.061                    |
| Cu      | 0.03                       | 0.03                     | 0.03                     |
| Al      | 0.001                      | 0.005                    | 0.025                    |
| S       | 0.008                      | 0.004                    | 0.004                    |
| P       | 0.017                      | 0.009                    | 0.011                    |
| N       | 0.021                      | 0.054                    | 0.054                    |
| O       | 0.011                      | 0.005                    | 0.004                    |

<sup>a</sup>Elements in wt. %.

ment produces a bcc solid solution containing dislocations and carbide precipitates. The lattice parameter of a ternary Fe-9 Cr-1 Mo alloy was found to be 28.74 nm. This value was employed in estimating the effects of point defect scattering on the phonon conductivity component.

### 3. EXPERIMENTAL VALUES

The absolute Seebeck coefficient values are shown in Fig. 1 and smoothed electrical resistivity and thermal conductivity data are shown in Table II. The procedure used to smooth the data has been described elsewhere [4] and the values shown in Table II are quoted with more digits than justified by the experimental uncertainty to eliminate rounding errors.

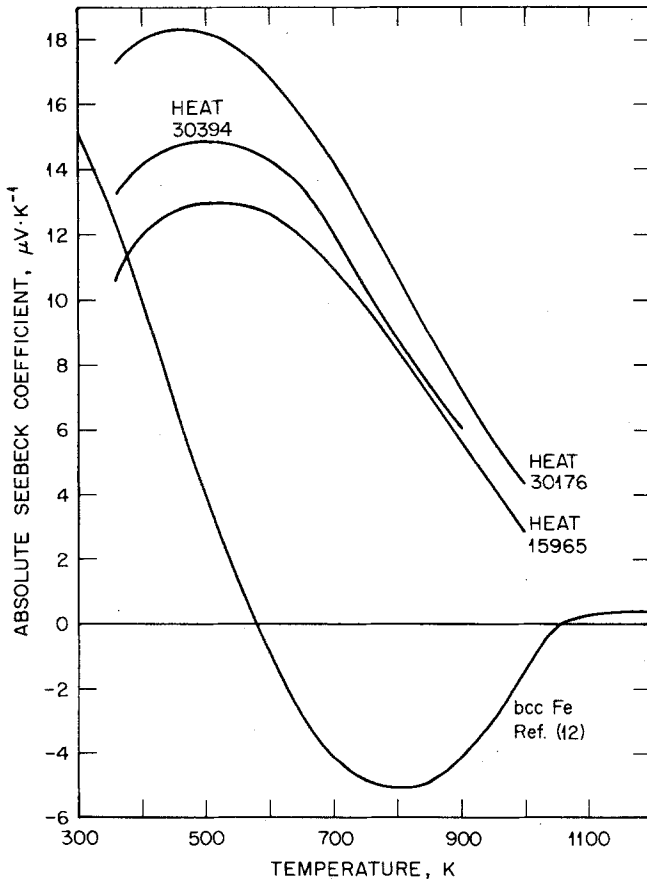


Fig. 1. Temperature dependence of the absolute Seebeck coefficient of three heats of 9 Cr-1 Mo steel.

Table II. Smoothed Thermal Conductivity  $\lambda$  and Electrical Resistivity  $\rho$  Values for Three Heats of 9 Cr-1 Mo Steel

| Temperature<br>(K) | Heat 15965  |  |   | Heat 30176                                   |   |  | Heat 30394  |  |  |
|--------------------|---|--|---|--|---|--|---|--|--|
|                    | $\lambda$<br>( $\text{W} \cdot \text{m}^{-1} \cdot \text{K}^{-1}$ ) | $\rho$<br>( $10^{-8}\Omega \cdot \text{m}$ ) | $\lambda$<br>( $\text{W} \cdot \text{m}^{-1} \cdot \text{K}^{-1}$ ) | $\rho$<br>( $10^{-8}\Omega \cdot \text{m}$ ) | $\lambda$<br>( $\text{W} \cdot \text{m}^{-1} \cdot \text{K}^{-1}$ ) | $\rho$<br>( $10^{-8}\Omega \cdot \text{m}$ ) | $\lambda$<br>( $\text{W} \cdot \text{m}^{-1} \cdot \text{K}^{-1}$ ) | $\rho$<br>( $10^{-8}\Omega \cdot \text{m}$ ) |  |
| 360                | 25.09   | 62.35  | 30.33   | 49.89  | 27.02   | 56.85  |   |  |  |
| 400                | 25.50   | 65.30  | 30.41   | 53.48  | 27.48   | 59.93  |   |  |  |
| 500                | 26.64   | 72.79  | 30.57   | 62.45  | 28.44   | 67.76  |   |  |  |
| 600                | 27.42   | 80.39  | 30.66   | 71.37  | 28.96   | 75.76  |   |  |  |
| 700                | 27.65   | 88.06  | 30.56   | 80.27  | 28.87   | 83.86  |   |  |  |
| 800                | 27.53   | 95.80  | 29.93   | 89.16  | 28.38   | 92.11  |   |  |  |
| 900                | 26.97   | 103.78                                       | 29.05   | 98.23  | 27.48   | 100.64                                       |   |  |  |
| 1000               | 25.81   | 112.44                                       | 27.78   | 107.66                                       | <sup>a</sup>  | <sup>a</sup>                                 |   |  |  |

<sup>a</sup> Experiment terminated due to heater failure.

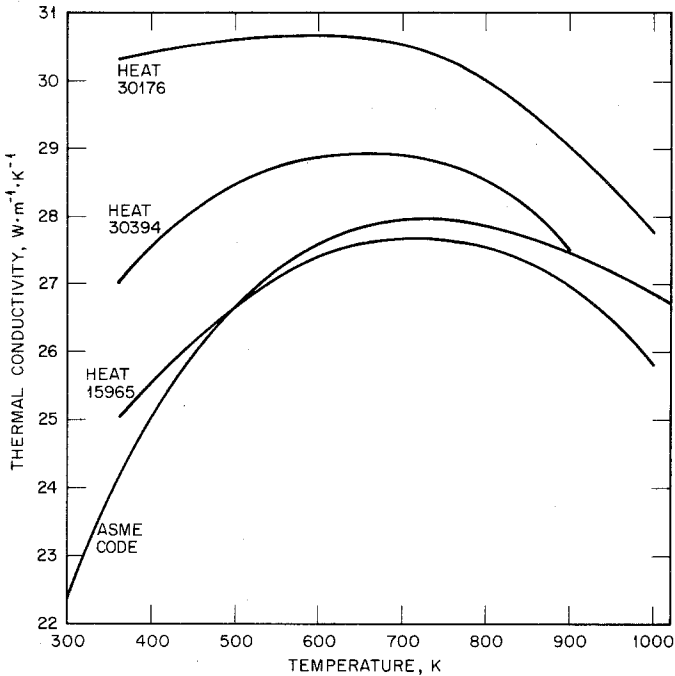


Fig. 2. Thermal conductivity data for three heats of 9 Cr-1 Mo steel. Values for the commercial heat (15965) agree with the ASME code.

The original error analysis [2] for the apparatus indicated maximum  $\lambda$  and  $\rho$  uncertainties of  $\pm 2.2$  and 0.4%, but tests with an Armco iron standard indicated that the  $\lambda$  uncertainty was somewhat larger at higher temperatures. The  $\lambda$  values for 9 Cr-1 Mo steel were therefore lowered [6] to force agreement with the Armco iron results. The maximum correction was  $-3.9\%$  at 1000 K. At 360 K the  $\lambda$  values for two heats (15965 and 30176) differ from data obtained by a comparative method [7] by  $-0.5$  and  $+1.8\%$ . The  $\lambda$  values for standard commercial and modified 9 Cr-1 Mo steel are compared with the ASME [8] code in Fig. 2. Our values for the commercial heat (15965) are in satisfactory agreement with the code and the data indicate that the modified alloy has an improved thermal conductivity.

#### 4. DISCUSSION

In an earlier publication [7] we showed that at room temperature the heat-to-heat variations in the  $\lambda$  and  $\rho$  of this steel correlated with differences in Si content. Figure 2 and Table II show that these trends persist

over the temperature range of this study, and the principal point of interest is to determine how well these trends can be understood in terms of available theory. An experimental identification of the electron  $\lambda_e$  and phonon  $\lambda_p$  components of the thermal conductivity of bcc Fe [4] is used as a basis for the analysis.

Except in certain special cases [9], the electronic thermal conductivity cannot be calculated from theory and must be obtained by using an appropriate electronic Lorenz function  $L(T)$  with the measured  $\rho$  values. We previously [4] showed that the  $L(T)$  and  $\lambda_p$  values obtained for bcc Fe at lower (100–400 K) temperatures could be extrapolated to higher temperatures to give a reasonably good account of the  $\lambda$  of Fe up to about 975 K. This  $L(T)$  was therefore assumed to apply to an intrinsic part of the  $\rho$  of the 9 Cr–1 Mo steels. The  $\lambda_e$  values for the alloys were then generated from the usual formula:

$$\lambda_e = \left[ \frac{\rho(\text{Fe})}{L(T)T} + \frac{\rho(\text{Alloy}) - \rho(\text{Fe})}{L_0 T} \right]^{-1} \quad (2)$$

In this equation  $L_0$  is the Sommerfeld value ( $2.443 \times 10^{-8} \text{ V}^2 \cdot \text{K}^{-2}$ ) and

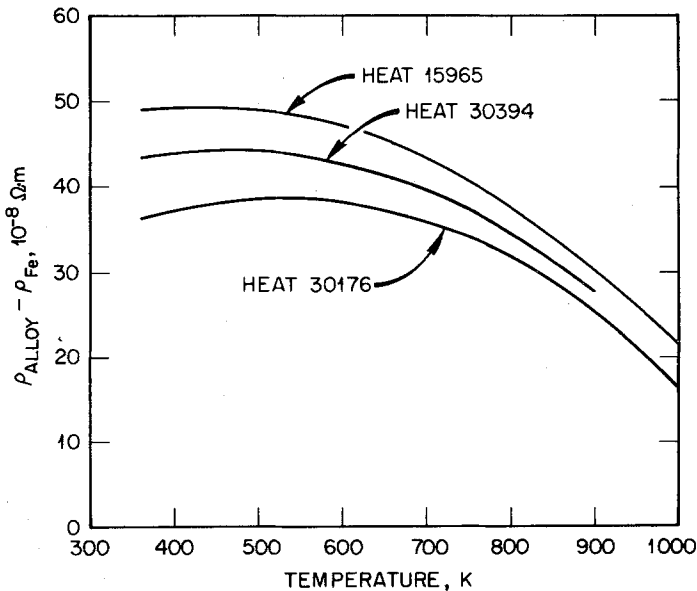


Fig. 3. The electrical resistivities of the steels do not obey Matthiessen's rule and the deviations are large.

$L(T)$ , which approaches  $L_0$  at high temperature, has been described [4] previously.

Figure 3 shows that the  $\rho$  of 9 Cr-1 Mo steel does not obey Matthiessen's rule, but this point may not affect the calculation of  $\lambda_e$  [10]. Large deviations are frequently observed in ferromagnetic alloys, and Bass [11] has summarized the theory.

The  $\lambda_e^{-1}$  curves for 9 Cr-1 Mo steel are shown in Fig. 4. At high temperatures they tend to approach the curve for bcc Fe, but the temperature dependence is much different. Reflecting the  $\rho$  differences, the  $\lambda_e$  calculated for the standard alloy is lower over the whole temperature range. This is attributed to its larger Si content.

Combining the  $\lambda_e$  values with the  $\lambda$  data (Table II) yields  $\lambda_p$  values for the three heats of 9 Cr-1 Mo steel. Values for  $\lambda_p^{-1}$  and some estimates for bcc Fe are shown in Fig. 5. The  $\lambda_p^{-1}$  curves for the alloys are higher but quite similar to the one for Fe and show that the trend with Si [7] content

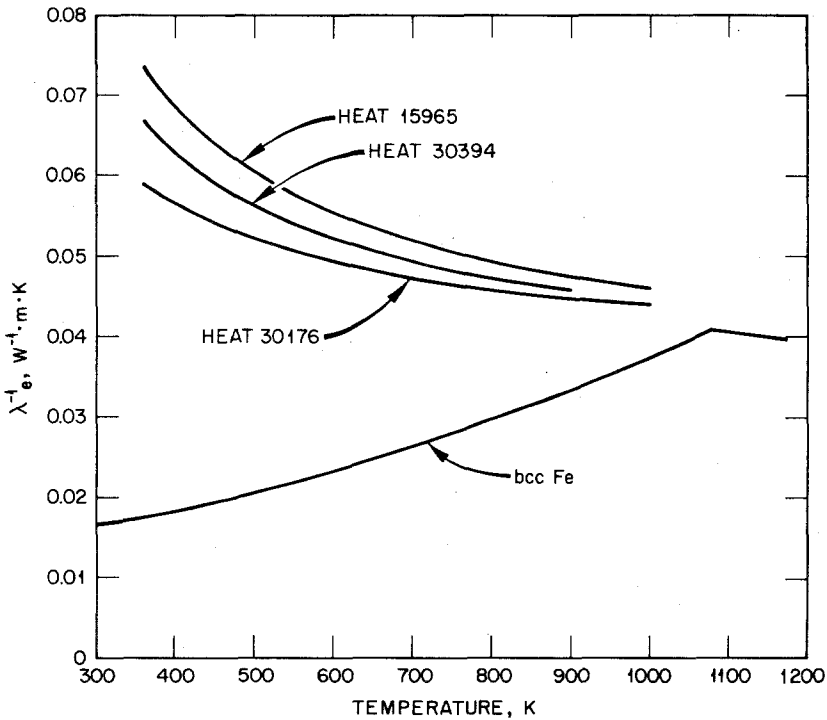


Fig. 4. Temperature dependence of the electronic thermal conductivity for three heats of 9 Cr-1 Mo steel.

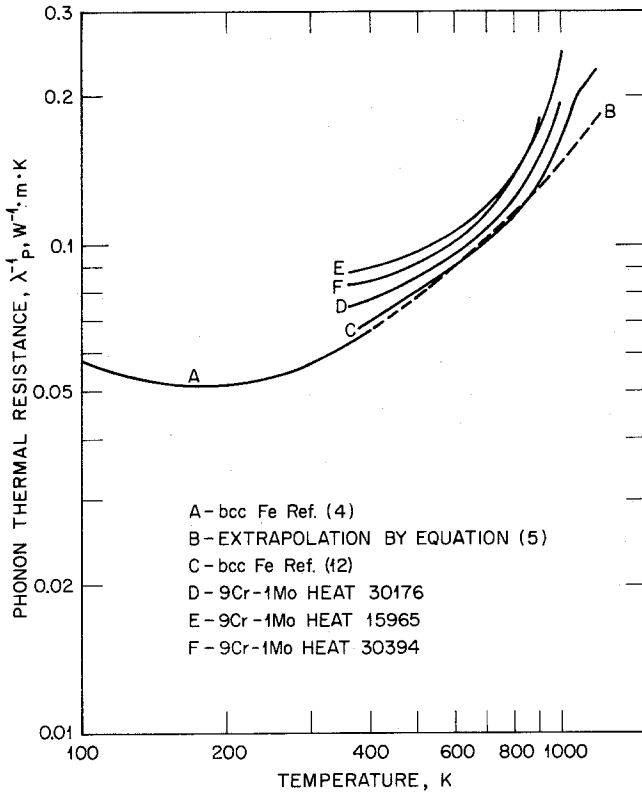


Fig. 5. Derived phonon thermal resistance values for bcc Fe and 9 Cr-1 Mo steel.

persists to higher temperatures. Rationalizing the information shown in Fig. 5 would demonstrate that the factors affecting the  $\lambda$  have been identified.

Examination of the curve for bcc Fe is a first step in this process. Figure 5 shows the  $\lambda_p^{-1}$  curve derived from low-temperature data (curve A) [4] and the result (curve C) obtained by combining  $\lambda$  data for high-purity and Armco iron [12] with the  $\lambda_e$  shown in Fig. 4. An extrapolation of the lower temperature values is also included (curve B). The low-temperature results for zone-refined Fe can be described by an equation containing phonon-phonon  $W_{pp}$  and electron-phonon  $W_{ep}$  resistance terms:

$$\lambda_p^{-1} = W_{pp} + W_{ep} = 9.86 \times 10^{-5} T + \frac{0.0269}{2} \left( \frac{418}{T} \right)^2 / J_3 \left( \frac{418}{T} \right) \quad (3)$$

When thermally induced volume changes become significant,  $W_{pp}$  increases



faster than  $T$ , and the extrapolation shown in Fig. 5 was obtained by adjusting the theoretical formula [13] to account for thermal expansion. This correction has been discussed elsewhere [14], and the formula used here includes the assumption that the Grüneisen constant  $\gamma_G$  varies with atomic volume  $V$  as

$$\frac{d \ln \gamma_G}{d \ln V} = 1.5 \gamma_G \quad (4)$$

Assuming a base temperature of 400 K and adjusting for changes in the Debye temperature  $\Theta_D$ ,  $\gamma_G$ , and the atomic volume, we obtain the following approximate high-temperature equation:

$$\lambda_p^{-1} = 9.86 \times 10^{-5} T [1 + \alpha_M (T - 400)(18\gamma_G - 1)] + 0.0269 \quad (5)$$

In this equation,  $\alpha_M$  is the mean linear thermal expansion coefficient and  $\gamma_G$  was presumed to equal 1.81 [15]. The numerical constant in Eq. (4) is not well known [14] and the  $W_{ep}$  term should also depend on temperature if the electronic density of states changes with temperature [16]. Despite this, Fig. 5 shows that, up to about 950 K, Eq. (5) is in good agreement with the  $\lambda_p^{-1}$  curve derived from  $\lambda$  and  $\lambda_e$  (curve C). Above this temperature, as the Curie temperature is approached, the difference between the two  $\lambda_p^{-1}$  curves suggests that an additional scattering process becomes significant. This effect is quite small and cannot be definitely established from the available data.

In the alloys, Fig. 5 shows that phonon energy transport is smaller than it is in pure Fe. Scattering from point defects (solute atoms) will always cause this kind of change. However, since the solute concentration is about 10 at %, changes in the phonon-phonon and electron-phonon scattering must also be considered. The Lindemann formula [15] can be used to estimate changes in the intrinsic phonon-phonon scattering, and this estimate indicates that  $W_{pp}$  is not significantly altered by alloying. Inspection of the curves shown in Fig. 5 also supports this assumption.

Alloying can either increase or decrease  $W_{ep}$  [17]. At present, the only method available for estimating these changes in bcc Fe alloy is based on a correlation [18] between  $W_{ep}$  and the electronic specific heat coefficient  $\gamma_e$ :

$$\lim_{T \rightarrow \infty} W_{ep} = 2.35 \times 10^{-3} \gamma_e^{1.5} \quad (6)$$

where  $\gamma_e$  is in units of  $\text{mJ} \cdot \text{K}^{-2} \cdot \text{mol}^{-1}$ . Using coefficients obtained from low-temperature specific heat data on binary Fe base alloys [19] yields

estimates of  $\gamma_e$  for the steels and these values average about 83% of the  $\gamma_e$  value for pure Fe [15, 19]. Thus, alloying should weaken the scattering of phonons by electrons, and this conclusion was included by making an additive resistance assumption:

$$\lambda_p^{-1}(\text{alloy}) = W + 2.35 \times 10^{-3} \gamma_e^{1.5}(\text{alloy}) \quad (7)$$

where  $W$  includes the effects of phonon-phonon and phonon-point defect scattering.

Demonstrating that the  $W$  values derived in this fashion can be predicted would show that the framework involving  $\lambda_e$ ,  $\lambda_p$ ,  $W_{ep}$ , and  $W$  is internally consistent. The ratio

$$\frac{W}{W_u} = \frac{(\lambda_p^{-1} - W_{ep})_{\text{alloy}}}{(\lambda_p^{-1} - W_{ep})_{\text{Fe}}} \quad (8)$$

should be given by a formula derived by Abeles [Ref. 20, Eq. (22)], which accounts for point defect scattering at high temperatures.

Using curve C of Fig. 5 to define  $W_u$  and Eq. (7) to calculate  $W_{ep}$  values for the alloys yields  $W$  versus temperature curves for the three samples. The theoretical calculations require values for the Debye temperature  $\Theta_D$ , the ratio of  $U$ - to  $N$ -process relaxation times  $\tau$ , and the total impurity scattering parameter  $\Gamma$ . The  $\Theta_D$  chosen, 418 K, is appropriate for intermediate temperatures [21].

The other two parameters,  $\tau$  and  $\Gamma$ , are to some extent interrelated, and  $\tau$  was fixed by selecting one particular theoretical equation [22] for  $\Gamma$  and finding that a  $\tau$  equal to 3 was required to yield satisfactory descriptions of experimental data for Ge-Si and III-V compound solid solutions [18].

The impurity scattering parameter  $\Gamma$  defines the phonon scattering strength of a specific solute, and has contributions from both mass-difference and local force-constant changes. It has been shown [23] that these contributions may either add or tend to cancel, and this was not included in Abeles' original paper. The formula employed here is due to Ho *et al.* [22],

$$\Gamma = \sum_L x_L \Gamma_L + \sum_H x_H \Gamma_H \quad (9)$$

where  $x$  is concentration, H and L are the number of heavy and light

solutes, respectively, and

$$\Gamma_L = \left( \frac{M_L - \bar{M}}{\bar{M}} + \gamma_G \frac{V_L - \bar{V}}{\bar{V}} \right)^2 \tag{10a}$$

$$\Gamma_H = \left( \frac{M_H - \bar{M}}{M_H} + \gamma_G \frac{V_H - \bar{V}}{\bar{V}} \right)^2 \tag{10b}$$

where  $\bar{M}$  and  $\bar{V}$  are the mass and atomic volume of virtual crystal atoms, respectively.

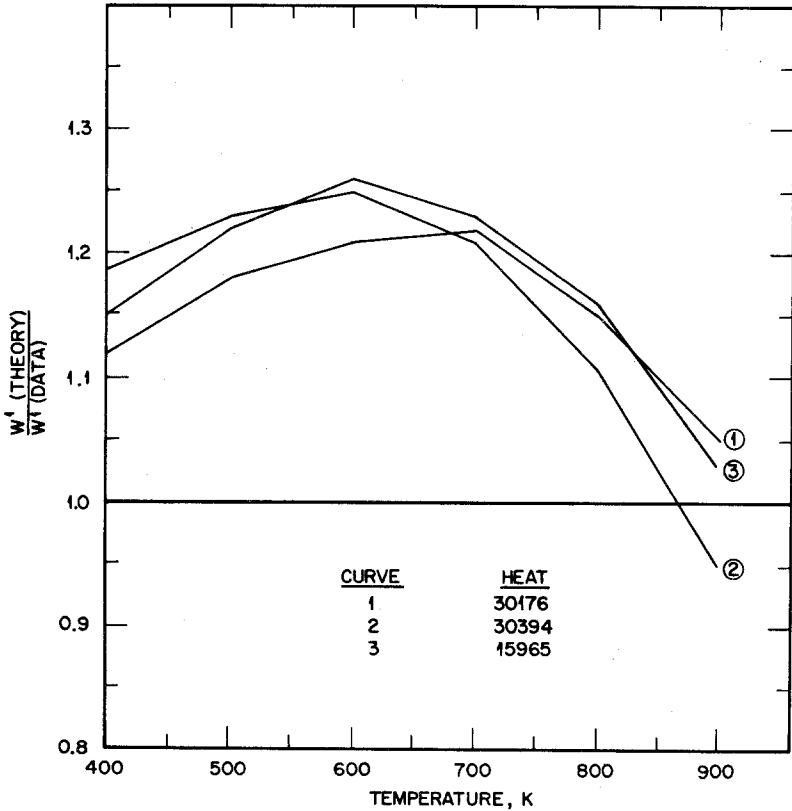


Fig. 6. Theoretical estimates of the effect of point-defect scattering on  $\lambda_p$  tend to overestimate the  $\lambda_p$  reduction.

The  $V_L$  and  $V_H$  are normally taken as equal to the atomic volume of the solute element, but this can lead to unrealistic estimates when the solute crystal lattice is more open than the solvent one. Silicon is one such case, since the diamond cubic lattice is much less close-packed than the bcc solvent, and lattice parameter measurements on bcc Fe-Si solutions indicate that Si atoms behave as if they were smaller than Fe atoms [24]. To include this, the  $\Gamma_{Si}$  and  $\Gamma_{Mo}$  values were obtained from the composition dependence of the lattice parameter [24]. These two terms contribute 90–95% of the point-defect scattering; and for Mo in bcc Fe, mass-difference scattering predominates.

The calculated and derived  $W$  values are compared in Fig. 6. This treatment overestimates the alloy scattering by an average of about 15% and the curves all show about the same temperature dependence. Since it includes  $W_{ep}$ , the  $\lambda_p$  estimates for the alloys are somewhat better and average about 90% of the derived (Fig. 5) values at 400 K.

This description is probably all that can be expected from the theory, since the strain scattering from Si is important and not well defined. Totally neglecting this contribution improves the agreement considerably, and improving the method used to calculate strain effects would be useful for understanding the significant role that Si plays in reducing the  $\lambda_p$  of bcc Fe solid solutions.

## ACKNOWLEDGMENTS

Research was sponsored by the Office of Breeder Technology Projects, Advanced Alloy Technology, U. S. Department of Energy, under contract W-7405-eng-26 with the Union Carbide Corporation. The comments of V. K. Sikka, which were based on his extensive experience with this alloy, are gratefully acknowledged. The manuscript was typed by C. Whitus and B. Hickey.

## REFERENCES

1. G. C. Bodine, Jr., B. Chakravarti, S. D. Harkness, B. Roberts, D. Vandergriff, and C. M. Owens, in *Ferritic Steels for Fast Reactor Steam Generators* (British Nuclear Society, London, 1978), pp. 160–164.
2. J. P. Moore, D. L. McElroy, and R. S. Graves, A Technique for Determining Thermal and Electrical Conductivity and Absolute Seebeck Coefficients between 300 and 1000 K, ORNL-4986 (1974).
3. R. S. Graves, R. K. Williams, and J. P. Moore, in *Thermal Conductivity 16* (Plenum Press, New York, 1983), pp. 343–349.
4. R. K. Williams, D. W. Yarbrough, J. W. Masey, T. K. Holder, and R. S. Graves, *J. Appl. Phys.* **52**:5167 (1981).

5. G. C. Bodine, Jr., B. Chakravarti, C. M. Owens, B. W. Roberts, D. M. Vandergriff, and C. T. Ward, A Program for the Development of Advanced Ferritic Alloys for LMFBR Structural Application, TR-MCD-015 (1977).
6. R. K. Williams, R. S. Graves, and J. P. Moore, A Study of the Effects of Several Variables on the Thermal Conductivity of 2 $\frac{1}{4}$  Cr-1 Mo Steel, ORNL-5313 (1978).
7. R. K. Williams, R. S. Graves, F. J. Weaver, and D. L. McElroy, in *Thermal Conductivity 17* (Plenum Press, New York, 1983), pp. 219-228.
8. *ASME Boiler and Pressure Vessel Code*, Section III, Table I-5.0 (ASME, New York, 1971), p. 413.
9. F. J. Pinski, P. B. Allen, and W. H. Butler, *Phys. Rev. B* **23**:5080 (1981).
10. P. G. Klemens, in *Thermal Conductivity 15* (Plenum Press, New York, 1978), pp. 203-207.
11. J. Bass, in *Advances in Physics* (Taylor and Francis, London, 1972), pp. 431-604.
12. W. Fulkerson, J. P. Moore, and D. L. McElroy, *J. Appl. Phys.* **37**:2639 (1966).
13. M. Roufosse and P. G. Klemens, *Phys. Rev. B* **7**:5379 (1973).
14. D. L. Mooney and R. G. Steg, *High Temp.-High Press.* **1**:237 (1969).
15. K. A. Gschneidner, Jr., *Solid State Phys.* **16**:275 (1964).
16. W. H. Butler and R. K. Williams, *Phys. Rev. B.* **18**:6483 (1978).
17. R. K. Williams, R. S. Graves, T. L. Hebble, D. L. McElroy, and J. P. Moore, *Phys. Rev. B* **26**:2932 (1982).
18. D. W. Yarbrough and R. K. Williams, Method for Estimating the Lattice Thermal Conductivity of Metallic Alloys, ORNL-5434 (1978).
19. S. Shinozaki, and A. Arrott, *Phys. Rev.* **152**:611 (1966).
20. B. Abeles, *Phys. Rev.* **131**:1906 (1963).
21. B. N. Brockhouse, H. E. Abou Helal, and E. D. Hallman, *Solid State Commun.* **5**:211 (1967).
22. C. Y. Ho, M. W. Ackerman, K. W. Wu, S. G. Oh, and N. J. Havill, *J. Phys. Chem. Ref. Data* **7**:959 (1978).
23. J. A. Krumhansl and J. A. D. Matthews, *Phys. Rev.* **140**:A1812 (1965).
24. W. B. Pearson, *A Handbook of Lattice Spacings and Structures of Metals and Alloys*, Vols. 1 and 2 (Pergamon Press, New York, 1958 and 1967).